



Published in final edited form as:

*J Am Chem Soc.* 2009 August 19; 131(32): 11387–11391. doi:10.1021/ja901875v.

## A New Gadolinium-based MRI Zinc Sensor

Ana C. Esqueda<sup>†</sup>, Jorge A. López<sup>†</sup>, Gabriel Andreu-de-Riquer<sup>†</sup>, José C. Alvarado-Monzón<sup>†</sup>, James Ratnakar<sup>‡</sup>, Angelo J. M. Lubag<sup>‡</sup>, A. Dean Sherry<sup>‡</sup>, and Luis M. De León-Rodríguez<sup>†,‡</sup>

<sup>†</sup> Departamento de Química. Universidad de Guanajuato, Cerro de la Venada s/n, Guanajuato, Gto., C.P. 36040, México Fax/Tel: 52 473-7326252

<sup>‡</sup> Advanced Imaging Research Center. University of Texas Southwestern Medical Center, 5323 Harry Hines Boulevard, Dallas, Texas 75390-9185, USA.

### Abstract

The properties of a novel Gd<sup>3+</sup>-based MRI zinc sensor are reported. Unlike previously reported Gd<sup>3+</sup>-based MRI contrast agents, this agent (GdL) differs in that the agent alone binds only weakly with human serum albumin (HSA) while the 1:2 GdL:Zn<sup>2+</sup> ternary complex binds strongly to HSA resulting in a substantial, three-fold increase in water proton relaxivity. The GdL complex is shown to have a relatively strong binding affinity for Zn<sup>2+</sup> ( $K_D = 33.6$  nM), similar to the affinity of the Zn<sup>2+</sup> ion with HSA alone. The agent detects as little as 30  $\mu$ M Zn<sup>2+</sup> in the presence of HSA by MRI *in vitro*, value slightly more than the total Zn<sup>2+</sup> concentration in blood ( $\sim 20$   $\mu$ M). This combination of binding affinity constants and the high relaxivity of the agent when bound to HSA suggests that this new agent may be useful for detection of free Zn<sup>2+</sup> ions *in vivo* without disrupting other important biological processes involving Zn<sup>2+</sup>.

### Introduction

Zinc is the second most abundant trace element (after iron) in mammalian tissues (the average adult human has ca. 3 grams of zinc).<sup>1</sup> Zinc exists exclusively as a divalent ion (Zn<sup>2+</sup>) in biology with most Zn<sup>2+</sup> bound to proteins that play a pivotal role in controlling gene transcription and metalloenzyme function.<sup>2</sup> Today, there is broad awareness of Zn<sup>2+</sup> signaling with a dozen or more individual zinc-secreting cell types known.<sup>3</sup> These include cells in the submandibular salivary gland, the pancreatic  $\beta$ -cells and pancreatic exocrine cells, the prostate epithelial cells, Paneth cells in the intestine, mast cells, granulocytes, pituitary cells and CNS neurons.<sup>4</sup> Zn<sup>2+</sup> is present in particularly high concentrations in the mammalian prostate, pancreas and brain. In addition to modulating neuronal transmission in brain, Zn<sup>2+</sup> is reported to contribute to neuronal injury in certain acute conditions, to suppress or induce apoptosis, and to induce the formation of  $\beta$ -amyloid ( $\beta$ A),<sup>5</sup> which is reported to be related to the etiology of Alzheimer's disease.<sup>6,7</sup> A considerable amount of data now shows that Zn<sup>2+</sup> and other metal ions (iron and copper) contribute to formation of  $\beta$ A deposits in the brain.<sup>8</sup> Concentrations as high as 0.2 to 1 mM of Zn<sup>2+</sup> have been found in amyloid plaques. It is also known that pancreatic  $\beta$ -cells release free chelatable Zn<sup>2+</sup> simultaneously with release of insulin such that the local concentration of Zn<sup>2+</sup> surrounding activated  $\beta$ -cells may be as high as 0.48 mM.<sup>9</sup> Thus,

lmdeleon@quijote.ugto.mx.

#### Supporting Information Available.

General experimental details; full experimental details including synthetic and characterization data for compound **3**, and its Gd<sup>3+</sup> and Eu<sup>3+</sup> complexes; full experimental details for fluorescence displacement experiments, relaxivity measurements, data fitting, modeling programs and mathematical derivations are provided. A proposed model figure of the binding of the CA to HSA is also included. This information is available free of charge via the Internet at <http://pubs.acs.org>.

monitoring release of  $\text{Zn}^{2+}$  from  $\beta$ -cells *in vivo* is an important goal in understanding the etiology and treatment of diabetes.<sup>10</sup>

Many disease conditions associated with either high or low  $\text{Zn}^{2+}$  concentrations are still widely debated and although it is recognized that  $\text{Zn}^{2+}$  has many important cellular roles, its physiological significance is not completely understood. Several chemical  $\text{Zn}^{2+}$  sensors have been reported, most based on fluorescence detection.<sup>11</sup> While these have proven useful for monitoring  $\text{Zn}^{2+}$  fluctuations in cells, their *in vivo* application is limited by light penetration in tissue, light scattering, and toxic photobleached byproducts. To the best of our knowledge, detection of free  $\text{Zn}^{2+}$  *in vivo* has not been demonstrated to date. Among alternatives to optical methods, magnetic resonance imaging (MRI) is promising since this technique allows non-invasive high resolution imaging of opaque bodies and monitoring of dynamic processes. There is considerable interest in the development of MRI contrast agents (CAs) that respond to biological events.<sup>12</sup> Most MR contrast agents are based on gadolinium ( $\text{Gd}^{3+}$ ) complexes that increase the relaxation rate of water ( $r_1$ ) through exchange of a single  $\text{Gd}^{3+}$ -bound water molecule with bulk solvent. The design of responsive CAs is typically based on changes in one or more factors that control proton relaxation times - water access to the metal, rotational correlation times, metal bound water exchange rates - in response to a specific stimulus (eg. enzyme,<sup>13</sup> protein,<sup>14</sup> pH,<sup>15</sup> metal,<sup>16</sup> etc.). A few  $\text{Zn}^{2+}$ -specific MRI CAs have been reported previously. The first was reported by Nagano and coworkers<sup>17</sup> who prepared a  $\text{Gd}^{3+}$  complex based on the diethylenetriaminepentaacetic acid (DTPA) ligand bifunctionalized with N,N-bis(2-pyridyl-methyl) ethylene diamine (BPEN), a moiety that has shown to have a binding specificity for  $\text{Zn}^{2+}$  over other metals. The relaxivity of this complex decreased from  $6.1 \text{ mM}^{-1} \text{ s}^{-1}$  to  $4.0 \text{ mM}^{-1} \text{ s}^{-1}$  ( $25^\circ\text{C}$ , pH 8, 7T) in the presence of 1 equivalent of  $\text{Zn}^{2+}$ , presumably by restricting access of water to the  $\text{Gd}^{3+}$  coordination site. However, the relaxivity of this complex returned to its initial value when a second  $\text{Zn}^{2+}$  was bound so these features make this system unattractive for testing *in vivo*. The same authors also reported a modified version of the DTPA derivative wherein one of the pyridylmethyl groups was replaced by an acetate moiety. This resulted in a complex that responded to  $\text{Zn}^{2+}$  by changing its relaxivity from 4.8 to  $3.5 \text{ mM}^{-1} \text{ s}^{-1}$  ( $25^\circ\text{C}$ , pH 7.2, 7T) upon addition of one equivalent of  $\text{Zn}^{2+}$  with no further changes upon addition of a second equivalent of  $\text{Zn}^{2+}$ .<sup>18</sup> Although this was an improvement in one sense, both systems result in an “on-off” response or image darkening upon  $\text{Zn}^{2+}$  binding – clearly not an optimal situation. More recently, Meade and coworkers<sup>19,20</sup> reported an “off-on”  $\text{Zn}^{2+}$ -responsive agent derived from  $\text{GdDO3A}$ . In this agent, the metal water coordination site is occupied by a carboxylate group of a diaminoacetate moiety attached through the fourth amino group of the macrocycle. When the diaminoacetate binds  $\text{Zn}^{2+}$ , a water molecule then coordinates to the  $\text{Gd}^{3+}$  which translates in an increase in relaxivity from  $2.3$  to  $5.1 \text{ mM}^{-1} \text{ s}^{-1}$  ( $37^\circ\text{C}$ , pH 7.4, 60MHz), a much more favorable 120% change. When dissolved in blood serum, however, the change in relaxivity of this complex changed much less in response to  $\text{Zn}^{2+}$ , from  $5.8$  to  $7.7 \text{ mM}^{-1} \text{ s}^{-1}$ . Nevertheless, an *in vitro* study showed that  $100 \mu\text{M}$   $\text{Zn}^{2+}$  could be detected by MRI by this agent in buffer and a  $\text{Zn}^{2+}$  binding constant of  $240 \mu\text{M}$  was determined by using a fluorescence competition method. Given that one would like to detect  $\text{Zn}^{2+}$  at even lower levels *in vivo*, continued development of agents that respond to  $\text{Zn}^{2+}$  *in vivo* under physiological conditions is highly desirable.

## Results and discussion

$\text{Gd}^{3+}$ -based MRI contrast agents derived from DOTA-like macrocyclic ligands have advantages over their linear counterparts (DTPA) because of their higher thermodynamic stability and kinetic inertness. Previous work has shown that the  $\text{GdDTPA}$ -bisBPEN diamide agent (zero net charge) developed by Nagano forms a 1:2 complex with  $\text{Zn}^{2+}$  while the  $\text{EuDOTA}$ -bisBPEN-di-butyl tetraamide PARACEST sensor (+3 charge) only forms a 1:1 complex with  $\text{Zn}^{2+}$ .<sup>21</sup> These differences must reflect the differences in total charge on each

$\text{Ln}^{3+}$  complex. Given these trends, a decision was made to investigate the  $\text{Zn}^{2+}$  binding properties of GdDOTA-bisBPEN diamide (net positive charge), **3**.

**3** was prepared as outlined in Scheme 1. **1** was first obtained by using a previous published procedure following protection-derivatization-deprotection schemes.<sup>22</sup> **1** was then coupled with 2 equivalents of BPEN (**2**) via activation of the free carboxylic acids with HBTU. After product purification, the *tert*-butyl groups were removed yielding **3** in a 74% overall yield. The  $\text{Gd}^{3+}$  and  $\text{Eu}^{3+}$  complexes of **3** were prepared and further purified by HPLC.

The relaxivity of GdDOTA-diBPEN increased with addition of  $\text{Zn}^{2+}$ . In the absence of  $\text{Zn}^{2+}$ , the relaxivity of the complex was  $5.0 \pm 0.1 \text{ mM}^{-1}\text{s}^{-1}$  (37°C, pH 7.6 0.1M Tris buffer, 23 MHz) and this gradually increased to  $6.0 \pm 0.1 \text{ mM}^{-1}\text{s}^{-1}$  with addition of  $\text{Zn}^{2+}$  until two equivalents had been added (Figure 1). This shows that a 1:2 (Gd:Zn) complex is formed. These  $r_1$  values are similar in magnitude to other GdDOTA-bis-amide complexes previously reported.<sup>23</sup> The relaxivity of GdDOTA-diBPEN remained constant when dissolved in 0.1 M phosphate buffer over a period of 24 hours, indicating that the agent is stable in a biological medium.<sup>24</sup> The relaxivity of GdDOTA-diBPEN did not change upon addition of  $\text{Ca}^{2+}$  or  $\text{Mg}^{2+}$  but did increase to  $6.3 \pm 0.1 \text{ mM}^{-1}\text{s}^{-1}$  (37°C, pH 7.6 tris buffer, 23 MHz) with addition of two equivalents of  $\text{Cu}^{2+}$ . Like  $\text{Zn}^{2+}$ , the relaxivity did not increase beyond this value with further addition of  $\text{Cu}^{2+}$ . Given that GdDOTA-bis-amide complexes are known to display slower water exchange rates than required for optimal relaxivity, the small increases in relaxivity promoted by binding of either  $\text{Zn}^{2+}$  or  $\text{Cu}^{2+}$  likely reflect an increase in water and/or proton exchange rates, perhaps catalyzed by  $\text{Zn}^{2+}$ -bound hydroxy groups as previously found for the PARACEST-based  $\text{Zn}^{2+}$  sensor, EuDOTA-bisBPEN-di-butyl tetraamide<sup>21</sup> or by creating a more organized second sphere of water molecules (those bound to  $\text{Zn}^{2+}$  or  $\text{Cu}^{2+}$ ) in close proximity to the single  $\text{Gd}^{3+}$ -bound water molecule of the complex. The mechanistic differences that determine the relaxivity change in response to  $\text{Zn}^{2+}$  for GdDOTA-diBPEN (altering water or proton exchange) as compared to the DTPA derivative reported by Nagano and coworkers<sup>17</sup> ( $\text{Gd}^{3+}$  water coordination blockage when two BPEN units coordinate one  $\text{Zn}^{2+}$  above the  $\text{Gd}^{3+}$ ) might be explained by the difference in charges between these two  $\text{Gd}^{3+}$  complexes. In the former, the complex has a net positive charge while the later  $\text{Gd}^{3+}$  complex is neutral so that a 1:1  $\text{Zn}^{2+}$  complex formation involving both BPEN units placing  $\text{Zn}^{2+}$  above the  $\text{Gd}^{3+}$  is less electrostatically restricted compared to GdDOTA-diBPEN. MALDI-TOF spectra of the GdDOTA-diBPEN- $\text{Zn}^{2+}$  adduct showed two major peaks, *m/z* 1208 and 1108 assigned to GdDOTA- $\text{Zn}_2(\text{OH})_4\text{diBPEN}$  and GdDOTA- $\text{Zn}(\text{OH})_2\text{diBPEN}$ , respectively (See supporting information Fig.S1). The high resolution <sup>1</sup>H NMR spectrum of EuDOTA-diBPEN shows that both possible coordination isomers are present in solution, the square antiprismatic (SAP) and twisted square antiprismatic (TSAP) in an approximate 3:2 ratio (See supporting information Figure S2) and that this ratio does not change with addition of  $\text{Zn}^{2+}$ .

The apparent binding dissociation constant ( $K_D$ ) of GdDOTA- $\text{Zn}_2\text{diBPEN}$  was determined by a competitive assay using the commercially available fluorophore ZnAF-2F (See supporting information and Figure S3). This dye was chosen since it shares similar  $\text{Zn}^{2+}$  binding moieties as GdDOTA-diBPEN and binds the metal with high affinity ( $K_D = 5.5 \text{ nM}$ ).<sup>25</sup> Using the published dissociation constant for the dye, a binding constant of  $33.6 \pm 0.4 \text{ nM}$  was estimated for formation of GdDOTA- $\text{Zn}_2\text{diBPEN}$  (per BPEN binding unit). As a reference, a similar ligand, bis(6-pyridinylmethyl)amine has been reported to form 1:1 complexes with  $\text{Zn}^{2+}$  with a  $K_D$  of 26.9 nM.<sup>26</sup>

Given that GdDOTA-diBPEN has two aromatic rings per BPEN unit, a further study was performed to investigate possible interactions between the agent and human serum albumin (HSA), the most abundant protein in blood and cerebral spinal fluid. Since metal ion mediated binding of small molecules to albumin has been reported previously,<sup>27</sup> we also examined the

influence of  $\text{Zn}^{2+}$  on binding interactions between the agent and albumin. A titration experiment performed by measuring the relaxation rate of a solution of GdDOTA-diBPEN upon addition of fatty acid-free HSA showed that the agent alone binds only weakly with HSA possibly due to non-specific electrostatic interactions. Surprisingly, when 2 equivalents of  $\text{Zn}^{2+}$  were added to the agent prior to addition of HSA, a quite different result was obtained (Figure 3). In this case, binding of the agent to HSA was surprisingly strong and the relaxivity of GdDOTA-diBPEN increased from  $6.6 \pm 0.1 \text{ mM}^{-1}\text{s}^{-1}$  to  $17.4 \pm 0.5 \text{ mM}^{-1}\text{s}^{-1}$  when fully bound to the protein (Figure 2), a 165% increase. A similar increase in relaxivity was observed for the GdDOTA- $\text{Cu}_2$ diBPEN upon addition of HSA but no change was observed for the complex containing either  $\text{Ca}^{2+}$  or  $\text{Mg}^{2+}$ . The increase in relaxivity observed for GdDOTA- $\text{Zn}_2$ diBPEN when bound to HSA likely reflects a slower rotational correlation time ( $\tau_R$ ) for the complex when bound to the protein.

To determine the  $K_D$  of GdDOTA- $\text{Zn}_2$ diBPEN with HSA, the proton relaxation enhancement,  $\epsilon^*$  (equation 2 in supporting information) versus HSA concentration was then fitted to a single site-specific binding model<sup>28</sup> (equation 3 in supplementary information). The best fit to the model gave a  $K_D$  of  $42 \pm 9 \mu\text{M}$  for GdDOTA- $\text{Zn}_2$ diBPEN binding to HSA.

Fluorescent displacement experiments were performed using warfarin and dansylglycine as probes to determine whether GdDOTA- $\text{Zn}_2$ diBPEN binds at site 1 or 2 of subdomain IIA or IIIA of HSA.<sup>29</sup> As shown in Figure 4, there is a decrease in dansylglycine fluorescence when increasing amounts of GdDOTA- $\text{Zn}_2$ diBPEN are added which suggests that the complex binds HSA in site 2 of subdomain IIIA. The  $K_D$  for GdDOTA- $\text{Zn}_2$ diBPEN to HSA was determined from these displacement results by assuming one site binding (equations 4 and 5 in supplementary information).<sup>30</sup> The fitting of the data gave a  $K_D$  of  $48 \pm 6 \mu\text{M}$ , a value similar to that described above in the proton enhancement titration experiment. Similar experiments were performed using GdDOTA-diBPEN alone (no divalent metal ion) but no displacement of either fluorescent probe was observed.

Although non-metal ion mediated, previous reports of positively charged GdDOTA complexes that bind HSA in site 2 can be found in the literature but no definitive binding model has been provided.<sup>31</sup> To provide a model of how GdDOTA- $\text{Zn}_2$ diBPEN might bind to HSA, we first performed a structural analysis of site 2 using literature data. Site 2 comprises a largely pre-formed hydrophobic cavity ( $\sim 16 \text{ \AA}$  deep and  $\sim 8 \text{ \AA}$  wide with a radius curvature  $\sim 8.5 \text{ \AA}$ ) with distinct polar features. It contains a cationic group located close to one side of the entrance of the binding pocket (R410) but also contains S489, E382 and N386 located near the surface on the opposite side. Y411 is centered inside the cavity (as a reference site 1 contains a cluster of four cationic residues at the entrance of the cavity K195, K199, R218, R222). Unlike binding site 1 where the binding entrance is enclosed by subdomains IIB and IIIA, the entrance to site 2 is not encumbered and is exposed to solvent. It is also known that binding to this site is favored with compounds that are planar or near planar and that contain aromatic rings.<sup>32</sup> The fact that GdDOTA-diBPEN interacts only weakly with HSA, while  $\text{Zn}^{2+}$  enhances this binding interaction considerably indicates that  $\text{Zn}^{2+}$  complexation “locks” the two aromatic pyridine rings, making the  $\text{ZnBPEN}$  unit better configured to fit into the binding site. Presumably the agent might first interact with S489, E382 and N386 at one side of the entrance given its positive net charge and once inside the cavity, the hydroxyl group of Y411 may interact with the  $\text{Zn}^{2+}$  and thereby provide further binding stability (see supporting information Figure S4 for a molecular model depicting the binding of GdDOTA- $\text{Zn}_2$ diBPEN to HSA). With this model, it is reasonable to consider that the presence of R410 on the opposite side of the cavity restricts rotational freedom of the bound agent through the methylene units connecting BPEN to the GdDOTA moiety. This could explain the dramatic increase in relaxivity that is observed for the agent bound to HSA, similar to that previously reported for positively charged GdDOTA type complexes.<sup>31</sup>

*In vitro* MR images of GdDOTA-diBPEN at 9.4-T in the presence of various  $\text{Zn}^{2+}$  concentrations demonstrates that  $\text{Zn}^{2+}$  can be detected at concentrations as low as 30  $\mu\text{M}$  (Figure 5). Unlike  $\text{Zn}^{2+}$ , there were no discernible differences in image intensity for samples of GdDOTA-diBPEN with added  $\text{Ca}^{2+}$  or  $\text{Mg}^{2+}$  (not shown).

To determine the effectiveness of GdDOTA-diBPEN as a relaxation agent under physiological conditions, relaxivity measurements were also performed in human blood serum. In this case, the relaxivity increase upon addition of  $\text{Zn}^{2+}$  was smaller, from  $6.1 \pm 0.1 \text{ mM}^{-1}\text{s}^{-1}$  to  $8.6 \pm 0.1 \text{ mM}^{-1}\text{s}^{-1}$  (37°C, pH 7.6 Tris buffer, 23 MHz) than observed previously for the agent in the presence of fatty acid free HSA. Nevertheless, this 40% increase in relaxivity should still be enough to be detectable by MRI *in vivo* upon release of free  $\text{Zn}^{2+}$ .

Based upon the binding equilibrium constants between GdDOTA-diBPEN,  $\text{Zn}^{2+}$  and HSA (multiple equilibria) and the relaxivities of GdDOTA-diBPEN, GdDOTA- $\text{Zn}_2$ diBPEN and ternary GdDOTA- $\text{Zn}_2$ diBPEN-HSA, one should be able to make a reasonable prediction of the detection limits of the  $\text{Zn}^{2+}$  sensor system *in vivo*. The minimum requirement is that the agent should be able to sense free, chelatable  $\text{Zn}^{2+}$  released in response to a particular metabolic event or metabolic abnormality. The CA should have a relatively strong binding affinity for  $\text{Zn}^{2+}$  but not so strong that it interferes with other endogenous metabolic processes. Given that HSA (a main component in blood) has a binding affinity for  $\text{Zn}^{2+}$  of 29.5 nM<sup>33</sup> and if one assumes that the local extracellular concentration of free chelatable  $\text{Zn}^{2+}$  near excitable cells rises to at least 475  $\mu\text{M}$  (as predicted for pancreatic  $\beta$ -cells),<sup>9</sup> then one can project the ideal tissue concentration of the  $\text{Zn}^{2+}$  sensor required to detect such an increase. If one first assumes that a standard clinical dose of CA will be injected (0.1 mmol/kg corresponds to an average extracellular tissue concentration of  $\sim 500 \mu\text{M}$ ) and that [HSA] in blood is  $\sim 600 \mu\text{M}$ , then a multiple equilibrium model (see supporting information) using the binding constants reported here predicts a steady-state concentration of ternary GdDOTA- $\text{Zn}_2$ diBPEN-HSA complex of  $\sim 131 \mu\text{M}$  with 27% of the total agent bound to  $\text{Zn}^{2+}$ . Given the relaxivity values of the various GdL species in human blood serum, this would correspond to a relaxation rate change ( $\Delta R_1$ ) of  $0.31 \text{ s}^{-1}$  ( $\sim 10\%$ ) between a high  $\text{Zn}^{2+}$  situation (475  $\mu\text{M}$ ) and normal physiology ( $\sim 20 \mu\text{M}$   $\text{Zn}^{2+}$  in blood).<sup>34</sup> This change in relaxation rate would be easily detected in an image. Ideally, it would be preferable to use a much lower concentration of sensor at a level where the agent is essentially silent (no “background signal”) under normal physiological  $\text{Zn}^{2+}$  levels but then increases upon  $\text{Zn}^{2+}$  release from tissues. The lowest concentration of agent required to detect 475  $\mu\text{M}$  of  $\text{Zn}^{2+}$  can be determined by extrapolating the previous calculation to a  $\Delta R_1$  of  $0.07 \text{ s}^{-1}$ , which is the predicted detection minimum of a targeted GdL sensor reported recently.<sup>35</sup> The calculated value corresponds to 50  $\mu\text{M}$  GdDOTA-diBPEN (Figure 6A) which coincides with the actual “silent” sensor condition of 50  $\mu\text{M}$  GdDOTA-diBPEN in human blood serum. So, given the relaxivity and binding characteristics of the  $\text{Zn}^{2+}$  sensor reported here, one would anticipate being able to inject only minimal amounts of sensor (50  $\mu\text{M}$ ) and still detect increases in  $\text{Zn}^{2+}$  concentrations approaching those expected for excitable cells. A second question that can be addressed using this same model is how important is the binding affinity between the sensor and  $\text{Zn}^{2+}$  for it to be useful *in vivo*? Figure 6B illustrates the estimated fractional amount of sensor- $\text{Zn}^{2+}$  complex formed with 500  $\mu\text{M}$  sensor and the indicated amount of total  $\text{Zn}^{2+}$  for four different binding constants. If one again uses a  $\Delta R_1$  of  $0.07 \text{ s}^{-1}$  as the lower limit of detection (this corresponds to  $\sim 6\%$  of the total agent bound to  $\text{Zn}^{2+}$ ), then one predicts that a sensor with a  $K_{\text{DGdLZn}} = 1 \mu\text{M}$  would only detect changes in  $\text{Zn}^{2+}$  concentration approaching 500  $\mu\text{M}$  while a sensor with a  $K_{\text{DGdLZn}} = 33.6 \text{ nM}$  (the agent reported herein) should detect changes in  $\text{Zn}^{2+}$  as low as  $\sim 100 \mu\text{M}$ . This highlights the importance of the  $\text{Zn}^{2+}$  binding constant in the *in vivo* study.

## Conclusions

A novel GdDOTA-based Zn<sup>2+</sup> sensor is reported that displays only a modest relaxivity increase upon binding to two equivalents of Zn<sup>2+</sup> but shows a substantially larger increase in relaxivity (165%) when the ternary GdL-Zn<sup>2+</sup> complex is bound to HSA. The Zn<sup>2+</sup> sensor does not respond to either Ca<sup>2+</sup> or Mg<sup>2+</sup> but does show a similar relaxation enhancement in the presence of Cu<sup>2+</sup>. This competition however would likely not interfere *in vivo* because Cu<sup>2+</sup> is typically found at much lower concentrations in tissues compared to Zn<sup>2+</sup>. *In vitro* imaging studies indicate that the present agent can detect Zn<sup>2+</sup> at concentrations as low as ~30 μM in presence of HSA. Further analysis shows that the binding dissociation constant of any CA to Zn<sup>2+</sup> with relaxivities in serum close to the agent presented herein should be at least 1 μM if the goal is to apply such systems *in vivo*.

## Supplementary Material

Refer to Web version on PubMed Central for supplementary material.

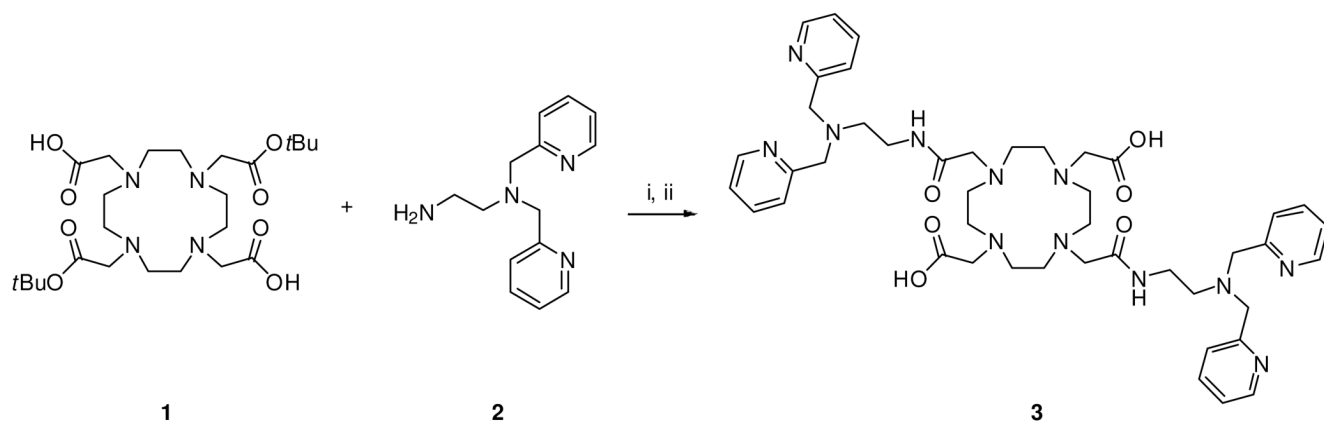
## Acknowledgements

The completion of this work was possible due to the support of CONACYT, Mexico sabbatical fellowship 75381 and by NIH grant DK-058398.

## References

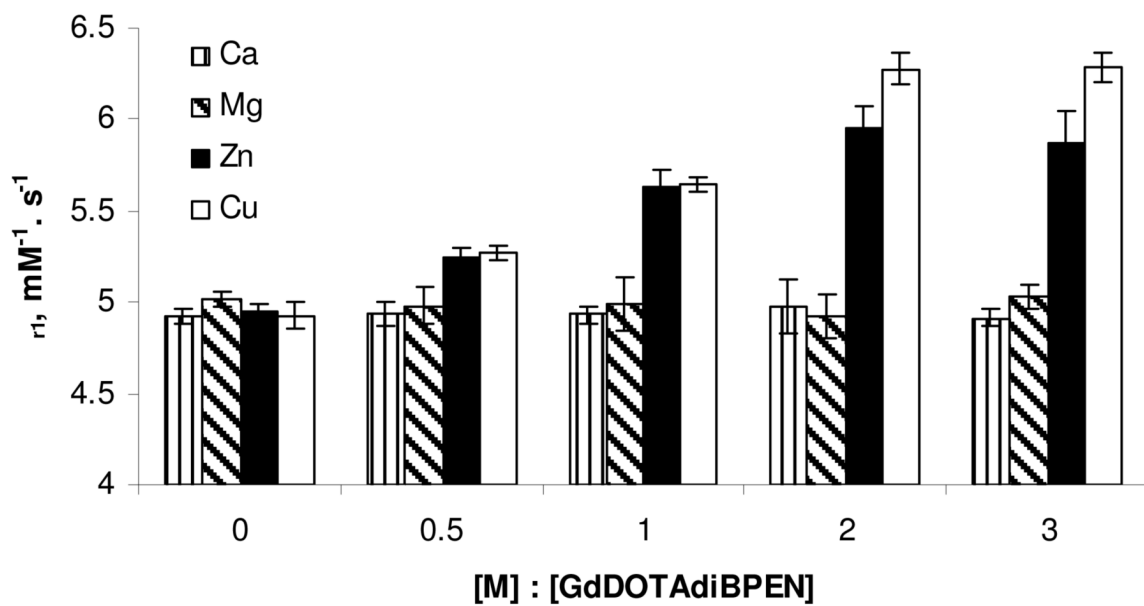
1. Mills, CF. Zinc in Human Biology. Springer-Verlag; New York: 1989.
2. Auld DS. BioMetals 2001;14:271–313. [PubMed: 11831461]
3. Frederickson CJ, Perez-Clausell J, Danscher G. J. Histochem. Cytochem 1987;35:579–83. [PubMed: 2435783]
4. Thompson RB, Peterson D, Mahoney W, Cramer M, Maliwal BP, Suh SW, Frederickson C, Fierke C, Herman P. J. Neurosci. Methods 2002;118:63–75. [PubMed: 12191759]
5. Mocchegiani E, Bertoni-Freddari C, Marcellini F, Malavolta M. Prog. Neurobiol 2005;75:367–90. [PubMed: 15927345]
6. Hardy J, Selkoe DJ. Science 2002;297:353–6. [PubMed: 12130773]
7. Hardy J. Curr. Alzheimer Res 2006;3:71–3. [PubMed: 16472206]
8. Frederickson CJ, Koh JY, Bush AI. Nat. Rev. Neurosci 2005;6:449–62. [PubMed: 15891778]
9. Kim BJ, Kim YH, Kim S, Kim JW, Koh JY, Oh SH, Lee MK, Kim KW, Lee MS. Diabetes 2000;49:367–372. [PubMed: 10868957]
10. Chausmer AB. J. Am. Coll. Nutr 1998;17:109–115. [PubMed: 9550453]
11. Kikuchi K, Komatsu K, Nagano T. Curr. Opin. Chem. Biol 2004;8:182–91. [PubMed: 15062780]
12. De Leon-Rodriguez LM, Lubag AJM, Malloy CR, Martinez GV, Gillies RJ, Sherry AD. Acc. Chem. Res., ASAP.
13. Louie AY, Huber MM, Ahrens ET, Rothbacher U, Moats R, Jacobs RE, Fraser SE, Meade TJ. Nat. Biotechnol 2000;18:321–5. [PubMed: 10700150]
14. De Leon-Rodriguez LM, Ortiz A, Weiner AL, Zhang S, Kovacs Z, Kodadek T, Sherry AD. J. Am. Chem. Soc 2002;124:3514–3515. [PubMed: 11929234]
15. Zhang S, Wu K, Sherry AD. Angew. Chem., Int. Ed 1999;38:3192–3194.
16. Li WH, Fraser SE, Meade TJ. J. Am. Chem. Soc 1999;121:1413–1414.
17. Hanaoka K, Kikuchi K, Urano Y, Nagano T. J. Chem. Soc., Perkin Trans 2001;2:1840–1843.
18. Hanaoka K, Kikuchi K, Urano Y, Narazaki M, Yokawa T, Sakamoto S, Yamaguchi K, Nagano T. Chem. Biol 2002;9:1027–1032. [PubMed: 12323377]
19. Major JL, Parigi G, Luchinat C, Meade TJ. Proc. Natl. Acad. Sci. U. S. A 2007;104:13881–13886. [PubMed: 17724345]
20. Major JL, Boiteau RM, Meade TJ. Inorg. Chem 2008;47:10788–10795. [PubMed: 18928280]

21. Trokowski R, Ren J, Kalman FK, Sherry AD. *Angew. Chem., Int. Ed* 2005;44:6920–3.
22. De Leon-Rodriguez LM, Kovacs Z, Esqueda-Oliva AC, Miranda-Olvera AD. *Tetrahedron Lett* 2006;47:6937–6940.
23. Zhang S, Kovacs Z, Burgess S, Aime S, Terreno E, Sherry AD. *Chem.--Eur. J* 2001;7:288–296.
24. Laurent S, Elst LV, Copoix F, Muller RN. *Invest. Radiol* 2001;36:115–22. [PubMed: 11224760]
25. Hirano T, Kikuchi K, Urano Y, Nagano T. *J. Am. Chem. Soc* 2002;124:6555–6562. [PubMed: 12047174]
26. Livieri M, Mancin F, Saielli G, Chin J, Tonellato U. *Chem.--Eur. J* 2007;13:2246–2256.
27. Klotz IM, Loh Ming W-C. *J. Am. Chem. Soc* 1954;76:805–814.
28. Mildvan AS, Cohn M. *Biochemistry* 1963;2:910–919. [PubMed: 14087380]
29. Krach-Hansen U, Chuang VTG, Otagiri M. *Biol. Pharm. Bull* 2002;25:695–704. [PubMed: 12081132]
30. Yung Chi C, Prusoff WH. *Biochem. Pharmacol* 1973;22:3099–3108. [PubMed: 4202581]
31. Montgomery CP, New EJ, Parker D, Peacock RD. *Chem. Commun* 2008:4261–3.
32. Ghuman J, Zunszain PA, Petitpas I, Bhattacharya AA, Otagiri M, Curry S. *J. Mol. Biol* 2005;353:38–52. [PubMed: 16169013]
33. Stewart AJ, Blindauer CA, Berezenko S, Sleep D, Sadler PJ. *Proc. Natl. Acad. Sci. U. S. A* 2003;100:3701–3706. [PubMed: 12598656]
34. Folin M, Contiero E, Vaselli GM. *BioMetals* 1994;7:75–9. [PubMed: 8118176]
35. Hanaoka K, Lubag AJM, Castillo-Muzquiz A, Kodadek T, Sherry AD. *Magn. Reson. Imaging* 2008;26:608–617. [PubMed: 18234462]

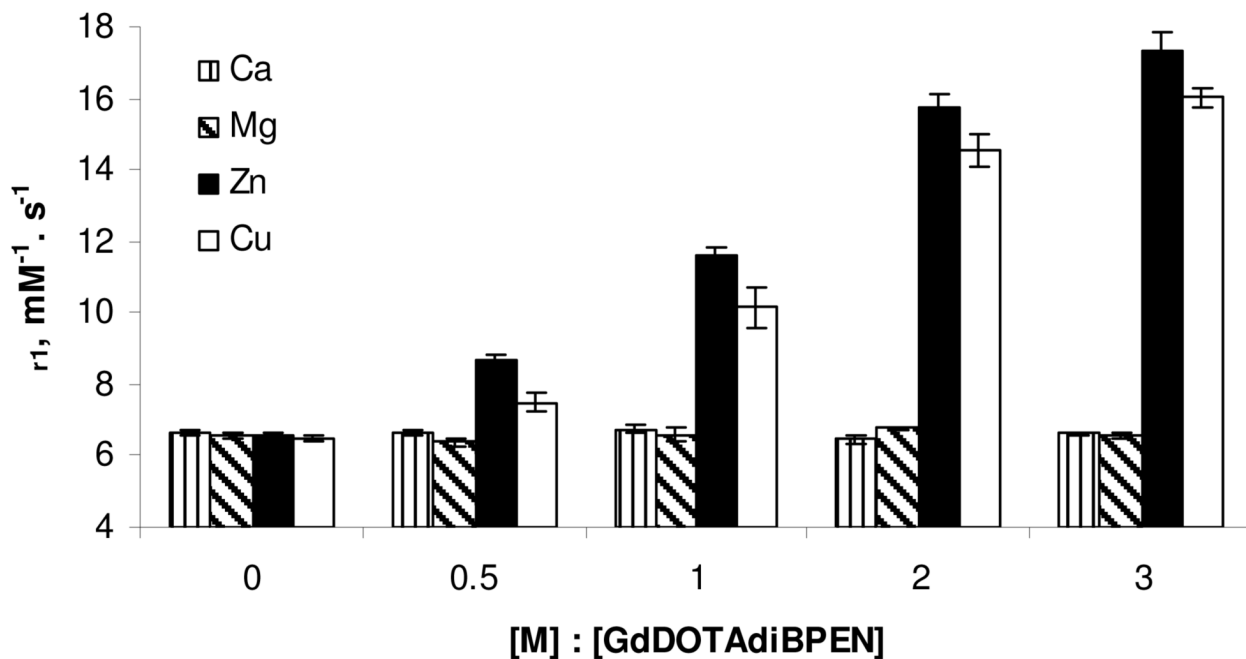


**Scheme 1.**  
i) HBTU, DMF, ii) TFA, DCM.

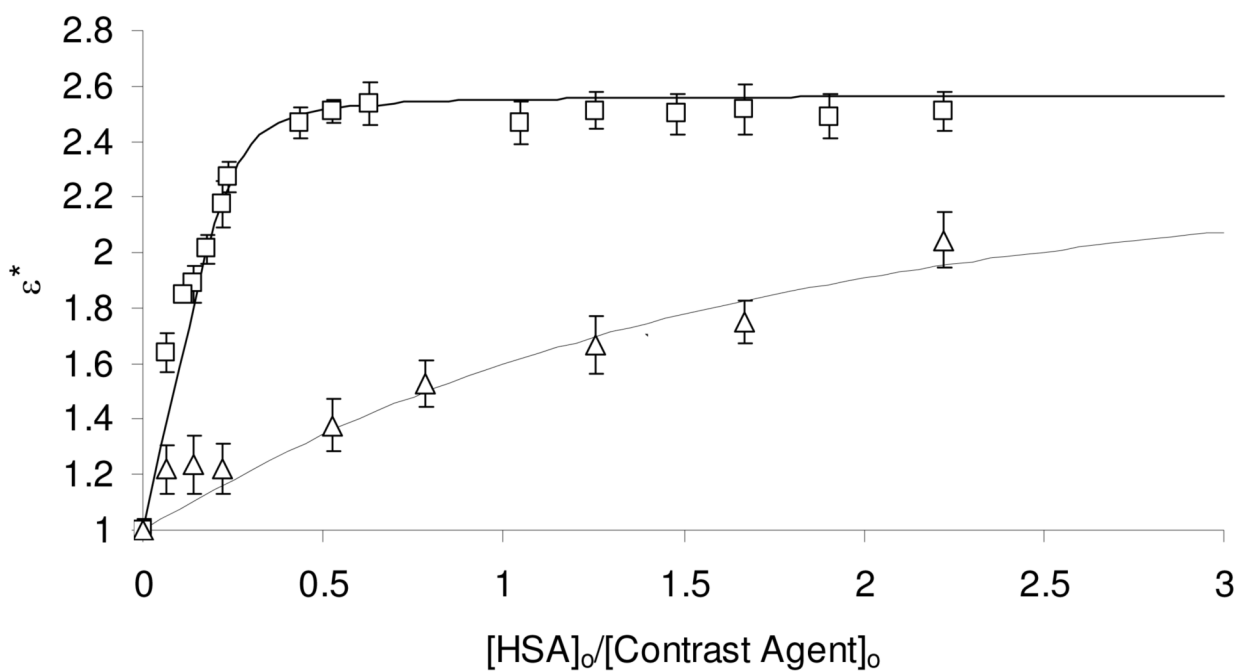




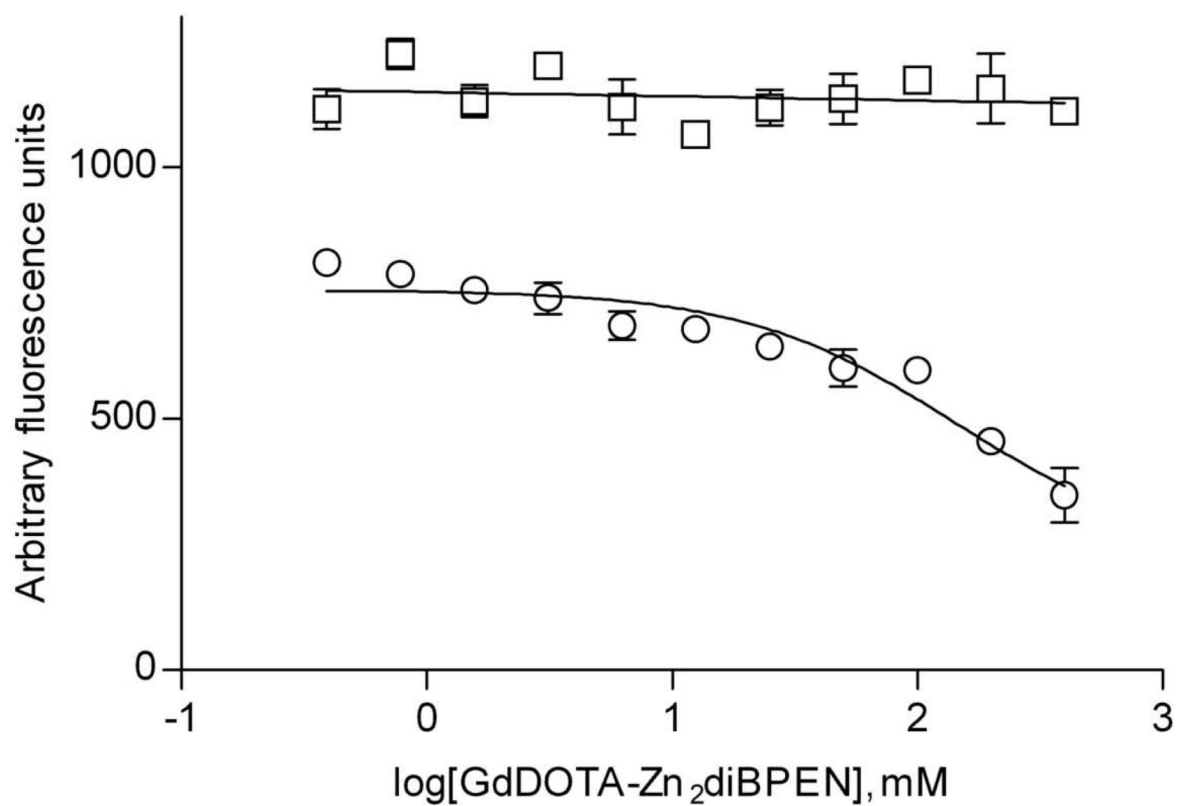
**Figure 1.** Relaxivity of GdDOTA-diBPEN at 23 MHz and 37°C in the presence of  $MCl_2$ , where  $M$  (=)  $Zn^{2+}$ ,  $Cu^{2+}$ ,  $Ca^{2+}$ , or  $Mg^{2+}$ . All solutions were prepared in 100 mM tris buffer at pH 7.6.



**Figure 2.** Relaxivity of GdDOTA-diBPEN at 23 MHz and 37°C in the presence of  $\text{MCl}_2$ , where M (=)  $\text{Zn}^{2+}$ ,  $\text{Cu}^{2+}$ ,  $\text{Ca}^{2+}$ , or  $\text{Mg}^{2+}$ . All solutions were prepared in 100 mM tris buffer at pH 7.6 plus 600  $\mu\text{M}$  human serum albumin (HSA).



**Figure 3.** Titration of GdDOTA-diBPEN 1 mM (triangles), and GdDOTA-diBPEN 1 mM plus 2 mM of Zn<sup>2+</sup> (squares) with HSA. All measurements were made at 23 MHz and 37° C in 100 mM tris buffer at pH 7.6. The solid curves represent the best fit to equation 3 in supporting information.

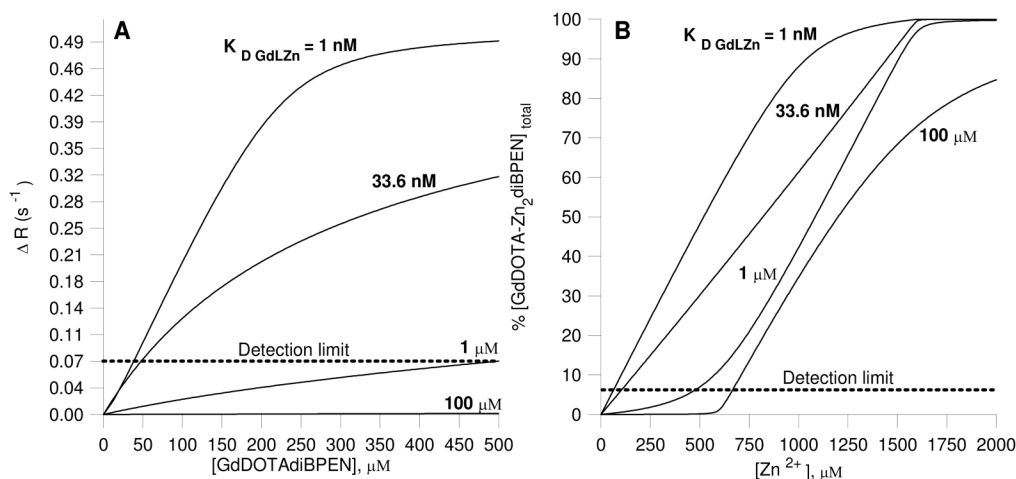


**Figure 4.** Displacement fluorescence plots for warfarin (squares, 5  $\mu$ M) and dansylglycine (circles, 5  $\mu$ M) from equimolar HSA by GdDOTA-Zn<sub>2</sub>diBPEN at 25°C in 100 mM tris buffer at pH 7.6. The solid curves represent the best fit to the data.



**Figure 5.**

$T_1$ -weighted phantom MR images. Images of a 100  $\mu\text{M}$  solution of GdDOTA-diBPEN in Tris buffer with 600  $\mu\text{M}$  HSA at various concentrations of  $\text{ZnCl}_2$ . Spot A, 200  $\mu\text{M}$  Zn; B, 100  $\mu\text{M}$  Zn; C, 30  $\mu\text{M}$  Zn; D, 0  $\mu\text{M}$  Zn; E, 600  $\mu\text{M}$  HSA but no contrast agent; F, Tris buffer only (no HSA or contrast agent). Repetition time (TR) = 200.0 ms; echo time (TE) = 8.3 ms; data matrix = 128 $\times$ 128. FOV = 15 $\times$ 15 mm<sup>2</sup>. Single scan, no averaging. A single slice of 5 mm was acquired centered at the sample height (10 mm). Window level and image size has been adjusted for printing purposes. Intensity scale is given in arbitrary units. Images and  $T_1$  values were obtained at 400 MHz (9.4 T).

**Figure 6.**

A. Calculated plots of  $\Delta R_1$  versus GdDOTAdiBPEN concentration for a 475  $\mu$ M  $Zn^{2+}$  rise from physiological conditions at various dissociation constants of the agent to  $Zn^{2+}$ . [HSA] = 600  $\mu$ M and relaxivity values were used as determined in blood serum. B. Calculated plots of the percent of total GdDOTA- $Zn_2$ BPEN relative to the initial concentration of unbound agent (500  $\mu$ M) versus the concentration of  $Zn^{2+}$  at various dissociation constants of the agent with  $Zn^{2+}$ . All other parameters were used as in A.